European Journal of Medicinal Chemistry Reports 5 (2022) 100045

HOSTED BY

Contents lists available at ScienceDirect

European Journal of Medicinal Chemistry Reports

journal homepage: www.editorialmanager.com/ejmcr/default.aspx

Rotenone enhances antifungal activity of novel pyrazoles against *Candida* spp.

Luis Fernando Quejada [a,b,c], Renata de Almeida [b,f], Percilene Fazolin Vegi [d], Maurício Silva dos Santos [e], Alice Maria Rolim Bernardino [d], Mauricio Afonso Vericimo [b,c,f], Robson Xavier Faria [c,g,*]

[a] *Proteomics and Human Mycosis Unit, Group of Infectious Diseases Department of Microbiology, Faculty of Sciences, Pontificia Universidad Javeriana, Carrera 7 No. 43-82, Bogotá, D.C, 110231, Colombia*
[b] *Laboratory of Immunology and Infectious and Granulomatous Diseases, Department of Biology, Fluminense Federal University, Niterói, RJ, Brazil*
[c] *Postgraduate Program in Science and Biotechnology, Fluminense Federal University, Niterói, RJ, Brazil*
[d] *Postgraduate Program in Chemistry, Institute of Chemistry, Fluminense Federal University, Niterói, RJ, Brazil*
[e] *Multicentric Postgraduate Program in Chemistry (PPGMQ-MG), Institute of Physics and Chemistry, Federal University of Itajubá, Itajubá, MG, Brazil*
[f] *Postgraduate Program in Pathology, Fluminense Federal University, Niterói, RJ, Brazil*
[g] *Toxoplasmosis and other Protozoa Laboratory, Oswaldo Cruz Institute, Oswaldo Cruz Foundation-FIOCRUZ, 21045-900, Rio de Janeiro, RJ, Brazil*

ARTICLE INFO

Keywords:
Invasive mycoses
Candida
Pyrazoles
Imidazolines
Rotenone
Antifungals

ABSTRACT

Mycoses annually affect about 2 million individuals worldwide, especially in tropical countries. *Candida* spp., one of the main etiologic agents of these mycoses, and in particular *Candida albicans* has been the most isolated pathogen in patients with severe clinical cases of invasive candidiasis and candidemia, causing frequent infections or opportunistic and chronic systemic forms. However, the emergence of non-albicans infections has become a public health concern worldwide. In discovering har.mless molecules, the pyrazoles have attracted many scientists because their great synthetic versatility and extensive therapeutic properties such as antibacterials, antivirals, antimalarials, and anti-inflammatories, anti-leishmaniasis, and antifungals. They are part of Azole compounds used for decades for antifungal treatment. The azole action mechanism is related to ergosterol synthesis inhibition by blocking the target enzymes, known as Erg11p, leading to fungistatic action. We evaluated the antifungal potential of 12 pyrazole derivatives. Compound **1d** caused prominent action against *Candida glabrata*. Thus, we employed Rotenone as a mitochondrial complex I inhibitor. Rotenone helped to enhance the effect of the novel pyrazole derivatives tested against *Candida* spp, decreasing MICs value from a range of 250–500 to <3.1 μg/mL. Pyrazoles had a reduced cytotoxicity effect on *in vivo* cell culture than ketoconazole. Although ROS production might be a possible mechanism, it remained unclear. Thus, new studies must elucidate this synergistic action.

1. Introduction

In recent decades, invasive fungal diseases have become very important in public health, especially those caused by *Candida* spp due to a ~40% mortality rate [1]. Historically, *Candida albicans* have been the most isolated pathogenic agents in patients with severe clinical cases of invasive Candidiasis and Candidemia [2–4]. However, non-albicans species, such as *C. parapsilosis*, *C. tropicalis*, and *C. glabrata*, with 58% Latin American cases [5,6]. Therefore, azole compounds such as Ketoconazole, Fluconazole, Itraconazole, and more recently, Voriconazole and Posaconazole have been the first line treatment for invasive candidiasis for years. Their "classic" mechanism of action is the blocking of the ergosterol synthesis, sterol needed for the functionality and fungal membrane fluidity through the enzyme lanosterol-14-α-demethylase inhibition, also called Erg11p [1,4,7]. Additionally, ROS (Reactive Oxygen Species) production stimulates lipid oxidation of the fungal cell. However, the azole-induced fungistatic effect in *Candida* spp has been shown to develop resistance rapidly by different resistance methods such as overexpression of the target site (ERG11) [7–9].

Intracellular ROS formation through aerobic respiration is a natural

* Corresponding author. Toxoplasmosis and other Protozoa Laboratory, Oswaldo Cruz Institute, Oswaldo Cruz Foundation-FIOCRUZ, 21045-900, Rio de Janeiro, RJ, Brazil.
E-mail addresses: lquejada@javeriana.edu.co (L.F. Quejada), salvador@ioc.fiocruz.br (R. Xavier Faria).

https://doi.org/10.1016/j.ejmcr.2022.100045
Received 1 December 2021; Received in revised form 19 March 2022; Accepted 3 April 2022
Available online 6 April 2022

process of eukaryotic cells, realized by mitochondrial complexes [10]. The disturbing of these complex functions trigger irreversible damage by the highly toxic ROS accumulation, leading to cytochrome *c* leakage and, consequently, apoptosis [11,12]. Rotenone is a complex I (NADH-Ubiquinone oxidoreductase) inhibitor which block proton pumping from the mitochondrial matrix. This compound is used as a pesticide and widely studied as a model of new therapies to treat diseases in humans. Previous works highlight the use of rotenone to potentiate the antifungal compound effect [13–15]. Rotenone uses in combination with azoles leads to a potent synergistic impact on fungal growth. Rotenone is well known for inducing ROS, carbonylation of proteins, and blocking proteasomal activity on mammalian cells [14,16].

Pyrazoles belong to the azole family with aromatic nitrogen heterocyclic rings in adjacent positions [17,18]. Pyrazole derivatives have become very important in recent years due to their chemical versatility and a broad spectrum of biological activity and therapeutic properties such as antiviral, antifungal [19], antibacterial [20], anti-inflammatory, antimalarial, antidepressant [21], and anticancer [22,23]. In the discovery of antifungals, numerous studies have reported mild to moderate effects against *Candida* spp. In non-*albicans* strains, the inhibitory action has been limited [24], behavior that was not different from the compounds tested in this work. However, the most relevant action has been achieved with *C. albicans*, as demonstrated by Mert et al. (2004) [25], where MIC values remained between 25 and 50 μg/mL. On the other hand, Vijesh et al. (2013) [26] obtained values between 6.25 and 25 μg/mL.

In this work, we evaluated the antifungal potential of new pyrazole derivatives on *Candida* spp and investigated the possible mechanism of action for pyrazole applicability in an experimental treatment.

2. Materials and methods

2.1. Compounds

2.1.1. Analytical techniques

All commercial raw materials and solvents were used as received. The progress of reactions was accomplished by thin-layer chromatography (TLC) on aluminum plates precoated with F254 silica gel. The melting points were determined on digital Fisatom 430 equipment. Fourier Transformer Infrared spectra (FT-IR) were recorded on Perkin-Elmer BX series FTIR spectrophotometer using KBr pellets. NMR spectra were recorded on a Varian Unity 300 MHz spectrometer in $CDCl_3$ or DMSO-d6 as solvent. The High-Resolution Mass Spectrometry (HRMS) was performed using Micromass/Waters ZQ-4000 spectrometer, Electrospray Ionization-ESI.

2.1.2. Synthesis of 5-amino-1-aryl-4-(4,5-dihydro-1H-imidazole-2-yl)-3-methyl-1H-pyrazoles 1(a-l)

To a solution of 5-amino-1-aryl-3-methyl-1*H*-pyrazoles **2(a–l)** (0.002 mol) in ethylenediamine (5 mL), at room temperature, was added dropwise cooled carbon disulfide (0.004 mol). After that, the reaction mixture was heated to 110–120 °C and then was maintained at this temperature range for 12–14 h. At the end of this time, the mixture was poured into crushed ice, the precipitate was filtered out and washed with cold water. After drying, the solid was obtained in good yields: 45–87%. All derivatives **2(a–l)** were previously published by our research group, except **2a** and **2f** which analytical results are showed below.

2.1.3. 5-amino-3-methyl-1-phenyl-1H-pyrazole (2a)

Yield: 73%; m.p.: 133–135 °C; FT-IR ν (cm^{-1}): 3332–3229, 2986–2867, 2218, 1597–1444; ^{1}H NMR (300 MHz, $CDCl_3$) δ 7.47–7.43 (m, 4H), 7.41 (t, J = 7,5 Hz, 1H), 4.56 (br, 2H), 2.32 (s, 3H); HRMS (ESI) m/z $[M+H]^+$ = 198.0901 (found), $[M+H]^+$ = 198.0905 (calculated).

2.1.4. 5-amino-1-(2′-chlorophenyl)-3-methyl-1H-pyrazole (2f)

Yield: 90%; m.p.: 193–195 °C; FT-IR ν (cm^{-1}): 3393–3278, 2987–2865, 2215, 1592–1437; ^{1}H NMR (400 MHz, $CDCl_3$) δ 7.48–7.41 (m, 3H), 7.57 (d, J = 7,6 Hz, 1H), 4.41 (br, 2H), 2.33 (s, 3H); HRMS (ESI) m/z $[M+H]^+$ = 232.0510 (found), $[M+H]^+$ = 232.0516 (calculated).***5-amino-3-methyl-1-phenyl-4-(4,5-dihydro-1H-imidazole-2-yl)-1H-pyrazole (1a)***

Yield: 59%; m.p.: 111–113 °C; FT-IR ν (cm^{-1}): 3357–3112, 2987–2863, 1603, 1597–1485; ^{1}H NMR (400 MHz, $CDCl_3$) δ 7.44–7.40 (m, 4H), 7.32–7.30 (m, 1H), 3.71 (s, 4H), 2.35 (s, 3H); HRMS (ESI) m/z $[M+H]^+$ = 242.1402 (found), $[M+H]^+$ = 242.1406 (calculated).

2.1.5. 5-amino-1-(3′-chlorophenyl)-4-(4,5-dihydro-1H-imidazole-2-yl)-3-methyl-1H-pyrazole (1b)

Yield: 79%; m.p.: 87–90 °C; FT-IR ν (cm^{-1}): 3357–3181, 2983–2858, 1605, 1599–1483; ^{1}H NMR (500 MHz, DMSO-d6) δ 7.74 (t, J = 2.0 Hz, 1H), 7.69 (ddd, J = 8.1, 2.0, 1.0 Hz, 1H), 7.64 (t, J = 8.1 Hz, 1H), 7.50 (ddd, J = 8.1, 2.0, 1.0 Hz, 1H), 6.93 (br, 2H), 3.61 (s, 4H), 2.41 (s, 3H); HRMS (ESI) m/z $[M+H]^+$ = 276.1008 (found), $[M+H]^+$ = 276.1016 (calculated).

2.1.6. 5-amino-1-(3′,5′-dichlorophenyl)-4-(4,5-dihydro-1H-imidazole-2-yl)-3-methyl-1H pyrazole (1c)

Yield: 45%; m.p.: 149–151 °C; FT-IR ν (cm^{-1}): 3308–3185, 2985–2869, 1610, 1587–1459; ^{1}H NMR (400 MHz, $CDCl_3$) δ 7.52 (d, J = 1.8 Hz, 2H), 7.29 (t, J = 1.8 Hz, 1H), 3.67 (s, 4H), 2.38 (s, 3H); HRMS (ESI) m/z $[M+H]^+$ = 310.0632 (found), $[M+H]^+$ = 310.0626 (calculated).

2.1.7. 5-amino-1-(3′,4′-dichlorophenyl)-4-(4,5-dihydro-1H-imidazole-2-yl)-3-methyl-1H-pyrazole (1d)

Yield: 87%; m.p.: 192–194 °C; FT-IR ν (cm^{-1}): 3440–3289, 2987–2863, 1605–1475; ^{1}H NMR (400 MHz, DMSO-d6) δ 7.93 (d, J = 2.5 Hz, 1H), 7.85 (d, J = 8.7 Hz, 1H), 7.72 (dd, J = 8.7, 2.5 Hz, 1H), 6.98 (br, 2H), 3.61 (s, 4H), 2.41 (s, 3H); HRMS (ESI) m/z $[M+H]^+$ = 310.0634 (found), $[M+H]^+$ = 310.0626 (calculated).

2.1.8. 5-amino-1-(4′-chlorophenyl)-4-(4,5-dihydro-1H-imidazole-2-yl)-3-methyl-1H-pyrazole (1e)

Yield: 76%; m.p.: 184–186 °C; FT-IR ν (cm^{-1}): 3367–3299, 2970–2860, 1600, 1593–1487; ^{1}H NMR (400 MHz, $CDCl_3$) δ 7.41–7.37 (m, 4H), 3.70 (s, 4H), 2.34 (s, 3H); HRMS (ESI) m/z $[M+H]^+$ = 276.1012 (found), $[M+H]^+$ = 276.1016 (calculated).

2.1.9. 5-amino-1-(2′-chlorophenyl)-4-(4,5-dihydro-1H-imidazole-2-yl)-3-methyl-1H-pyrazole (1f)

Yield: 76%; m.p.: 110–112 °C; FT-IR ν (cm^{-1}): 3462–3265, 2956–2859, 1615, 1595–1446; ^{1}H NMR (400 MHz, DMSO-d6) δ 7.77–7.75 (m, 1H), 7.61–7.57 (m, 3H), 6.51 (br, 2H), 3.60 (s, 4H), 2.38 (s, 3H); HRMS (ESI) m/z $[M+H]^+$ = 276.1010 (found), $[M+H]^+$ = 276.1016 (calculated).

2.1.10. 5-amino-1-(4′-fluorophenyl)-4-(4,5-dihydro-1H-imidazole-2-yl)-3-methyl-1H-pyrazole (1g)

Yield: 45%; m.p.: 167–169 °C; FT-IR ν (cm^{-1}): 3362–3189, 2957–2866, 1603, 1597–1487; ^{1}H NMR (400 MHz, DMSO-d6) δ 7.71–7.66 (m, 2H), 7.46–7.40 (m, 2H), 6,74 (br, 2H), 3.61 (s, 4H), 2.40 (s, 3H); HRMS (ESI) m/z $[M+H]^+$ = 260.1307 (found), $[M+H]^+$ = 260.1311 (calculated).

2.1.11. 5-amino-1-(3′-fluorophenyl)-4-(4,5-dihydro-1H-imidazole-2-yl)-3-methyl-1H-pyrazole (1h)

Yield: 65%; m.p.: 83–85 °C; FT-IR ν (cm^{-1}): 3352–3196, 1609, 1595–1452; ^{1}H NMR (400 MHz, DMSO-d6) δ 7.64–7.61 (m, 1H), 7.58–7.51 (m, 2H), 7.29–7.26 (m, 1H), 6.92 (br, 2H), 3.61 (s, 4H), 2.41 (s, 3H); HRMS (ESI) m/z $[M+H]^+$ = 260.1307 (found), $[M+H]^+$ = 260.1311 (calculated).

2.1.12. 5-amino-1-(2′-bromophenyl)-4-(4,5-dihydro-1H-imidazole-2-yl)-3-methyl-1H-pyrazole (1i)

Yield: 50%; m.p.: 102–103 °C; FT-IR ν (cm^{-1}): 3466–3266,

2958–2866, 1614, 1594–1444; ^{1}H NMR (400 MHz, DMSO-d6) δ 7.91 (dd, J = 8.0, 1.3 Hz, 1H), 7.64 (td, J = 7.8, 1.3 Hz, 1H), 7.56–7.51 (m, 2H), 6.43 (br, 2H), 3.60 (s, 4H), 2.38 (s, 3H); HRMS (ESI) m/z $[M+H]^+$ = 320.0516 (found), $[M+H]^+$ = 320.0511 (calculated).

2.1.13. 5-amino-1-(4′-bromophenyl)-4-(4,5-dihydro-1H-imidazole-2-yl)-3-methyl-1H-pyrazole (1j)

Yield: 71%; m.p.: 194–196 °C; FT-IR ν (cm^{-1}): 3363–3208, 2968–2859, 1597, 1581–1445; ^{1}H NMR (400 MHz, DMSO-d6) δ 7.78 (d, J = 9.3 Hz, *2*H), 7.65 (d, J = 9.3 Hz, *2*H), 6.84 (br, 2H), 3.62 (s, 4H), 2.41 (s, 3H); HRMS (ESI) m/z $[M+H]^+$ = 320.0515 (found), $[M+H]^+$ = 320.0511 (calculated).

2.1.14. 5-amino-1-(3′-bromophenyl)-4-(4,5-dihydro-1H-imidazole-2-yl)-3-methyl-1H-pyrazole (1k)

Yield: 56%; m.p.: 85–87 °C; FT-IR ν (cm^{-1}): 3357–3212, 1603, 1591–1449; ^{1}H NMR (400 MHz, DMSO-d6) δ 7.87 (t, J = 2.0 Hz, 1H), 7.73 (ddd, J = 8.0, 2.0, 1.0 Hz, 1H), 7,63 (ddd, J = 8.0, 2.0, 1.0 Hz, 1H), 7.56 (t, J = 8.0 Hz, 1H), 6.91 (br, 2H), 3.62 (s, 4H), 2.41 (s, 3H); HRMS (ESI) m/z $[M+H]^+$ = 320.0518 (found), $[M+H]^+$ = 320.0511 (calculated).

2.1.15. 5-amino-1-(4′-methoxyphenyl)-4-(4,5-dihydro-1H-imidazole-2-yl)-3-methyl-1H-pyrazole (1l)

Yield: 46%; m.p.: 146-146 °C; FT-IR ν (cm^{-1}): 3363–3208, 2964–2836, 1618, 1597–1447; ^{1}H NMR (400 MHz, DMSO-d6) δ 7.54 (d, J = 8,2 Hz, 2H), 7.16 (d, J = 8,2 Hz, 2H), 6.59 (br, 2H), 3.91 (s, 3H), 3.61 (s, 4H), 2.40 (s, 3H); HRMS (ESI) m/z $[M+H]^+$ = 272.1507 (found), $[M+H]^+$ = 272.1511 (calculated).

2.2. Microorganisms and culture

The yeast strains of *C. albicans* ATCC 24433, *C. albicans* ATCC 14053, *C. krusei* ATCC 6258, *C. parapsilosis* ATCC 22019, and *C. glabrata* MYA 2950 were obtained from Fiocruz in Rio de Janeiro, Brazil. All yeast were cultured on Sabouraud Dextrose Agar (Flukaanalytical) (40 g/L Dextrose, 10 g/L Peptone, 15 g/L Agar) and incubated at 35 °C for 24–72 h until growth was observed. The cultures were stored at −80 °C.

2.3. Disk diffusion antifungal test

The antifungal sensitivity test was performed according to the Kirk-Bauer methodology (CLSI) using filter paper disks soaked with 5 mg/mL pyrazole derivatives placed on a culture in a Petri dish. We obtained a cell suspension adjusted to the McFarland 0.25 scale. A 0.1 mL aliquot was pipetted into a Sabouraud agar petri dish and spread with a swab. The plates were maintained at 35 °C for 30 min, then the disks were placed on agar and impregnated with 20 μL of the compounds, and then the plates were incubated for 24 h at 35 °C.

The drug sensitivity was determined by measuring the diameter, of microbial growth inhibition zone in millimeters [27]. The disks soaked in dimethyl sulfoxide (DMSO) and Ketoconazole were negative and positive controls. Image J was used for the image analysis, and the image obtained data analysis in statistical software GraphPadPrism v.8.

2.4. Antifungal susceptibility testing

The antifungal susceptibility of the twelve pyrazole derivatives was tested using a modified protocol according to Clinical and laboratory standards (CLSI)M27-A3 standard guidelines [28]. Different concentrations in the range of 3,8–500 μg/mL were evaluated. The Minimum Inhibitory Concentration (MIC) was considered the lowest drug concentration to cause inhibition of growth compared to the drug-free growth control. The MIC was determined visually and supported by fluorescence measurements with resazurin (250 μg/mL) as a redox indicator. Resazurin is a blue non-toxic cell-permeable compound and virtually non-fluorescent. Upon entering living cells, resazurin is reduced to resorufin, a violet compound to pink and highly fluorescent [29].

2.5. Cytotoxicity assay

This procedure was performed under sterile conditions, and the cells were harvested in RPMI-1640 with 10% Bovine Fetal Serum (SFB). Subsequently, the cell count was performed under an optical microscope on the Neubauer hemocytometer, and the suspensions were adjusted for the test.

For cytotoxicity assay, this was performed according to Resazurin Protocol [30]. Cells were cultured in 96-well microplates at a 5×10^5 cells/mL concentration in the final volume of 100 μL per well. After a 24-h incubation period, necessary for cells to adhere to the plate, different pyrazole derivatives were added in the volume of 100 μL. As a control, only half was used. The microplate was then incubated in an oven at 37 °C at 5% CO_2 for 24 and 48 h. Cell viability was assessed colorimetric and supported by fluorescence measurements with a redox indicator of 20 μL resazurin (250 μg/mL). The plates were analyzed in a SpectraMax M4 spectrophotometer (Molecular Devices) at wavelengths 530, 570, and 586 nm to establish the CC_{50}/24 h values. The CC_{50} values (50% cytotoxic concentration) were determined by linear regression from three independent experiments.

2.6. Lactate dehydrogenase (LDH) release assay

LDH release was measured after treatment with 0.1 ng/mL – 250 μg/mL rotenone on mice peritoneal macrophages. A quantity of 2×10^5 peritoneal macrophages cells per well was treated for 24 h. No treated cells and cells treated with 0.1% Triton-X 100 represented the negative and positive controls, respectively. The supernatant extracted from the treatments of the 96-well plate is used for the detection of the LDH enzyme, according to the protocol (Doles, RJ, Brazil). After, the centrifugation at 1500 rpm for 10 min, the supernatant (10 μL) was placed on a second plate. We left the plate in the greenhouse for 10 min. The solution containing substrate (80 μL) + ferric alum (10 μL) was left in the oven for 5 min in a 35 mm Petri dish. This solution was added to supernatant (10 μL) and left in the oven for 5 min (37 °C). Next, Nicotinamide (NAD; 5 μL) was added to each well for 5 min in the dark. Posteriorly, a stabilizer solution (50 μL of 1 N Hydrochloric acid - HCl) was added. The white solution contains only the medium involved in the reaction. The sample was analyzed in a plate reading (λ = 510 nm) within 30 min afterward.

2.7. Determination of the effect of respiratory inhibitors on susceptibility

The effect of respiratory inhibitors on antifungal susceptibility was evaluated with Rotenone, Malonate, Sodium Azide, AntimycineA (AA), Oligomycine A (OA), and Potassium Cyanide (CNK) following microdilution in broth protocol as performed for MIC determination. In addition, two effective pyrazoles were assessed in the assay. Experiments were performed in triplicates. The results were analyzed as fluorescence units by the SpectraMax M4 spectrophotometer (Molecular Devices).

2.8. Measurement of intracellular ROS

Intracellular levels of ROS were measured with Dihydroethidium (DHE; Sigma Aldrich Ltd). Two concentrations of compounds were evaluated in this experiment; the MIC value and a sub-inhibitory concentration (65 μg/mL) of pyrazoles were added into 96 wells microplates with yeast suspension incubated at 35 °C/2 h. In addition, a 20 μL aliquot of a solution of DHE 10 nM was added 30 min before finishing incubation, as described by Farias et al., 2008 [31]. Fluorescence units were analyzed by the SpectraMax M4 spectrophotometer (Molecular Devices). A solution of 40 μg/mL (Sigma - Aldrich) was used as a positive control and drug-free as a negative control. All treatments were performed in triplicate.

2.9. Viability assay with ethidium bromide

From a Candida culture with 24 h of incubation in Sabouraud broth, the assay was prepared in a 96-well plate as described in the MIC determination. MIC value and a sub-inhibitory concentration (65 μg/mL) of pyrazoles were added into 96 wells microplates and incubated at 35 °C/2 h. An aliquot of 20 μL of a 50 nM ethidium bromide solution was added 30 min before ending the incubation. The fluorescence intensity was quantified at wavelengths 526 (excitation) - 605 nm (emission). Amphotericin B was used as a fungicidal control and culture without compounds as a negative control. The assay was also performed after 24 h of incubation. All treatments were performed in triplicate.

2.10. Statistical analysis

The fluorescence reading results, MIC with resazurin, ROS quantification with DHE, and nuclear fluorescence with ethidium bromide were tabulated and analyzed using analysis of variance (ANOVA), followed by the Tukey *t*-test using the program GraphPad Prism 8. Values with $p < 0.05$ were considered significant.

3. Results

3.1. Synthesis

The synthesis of planned compounds 5-amino-1-aryl-4-(4,5-dihydro-1*H*-imidazole-2-yl)- 3-methyl-1*H*-pyrazoles **1(a–l)** were performed in two steps (Scheme 1). Firstly, the corresponding arylhydrazine hydrochloride reacted with sodium acetate, in ethanol, under reflux. Then, (1-ethoxyethylidene) malononitrile was added, and the key intermediates 5-amino-1-aryl-3-methyl-1*H*-pyrazoles **2(a–l)** were obtained in good yields (54–95%) [32]. In the second step, a mixture of **2(a–l)**, ethylenediamine and carbon disulfide (CS_2) was reacted to synthesize the targets compounds **1(a–l)** (45–87% yield) [33].

3.2. Antifungal susceptibility of Candida spp.

Among 12 tested compounds, **1d and 1j** showed a discreet effect against three out five *Candida* spp. In particular, *Candida glabrata* resulted the most sensible yeast with a MIC in the range 250–500 μg/mL. In this assay, ketoconazole was used as a positive control. The values of MIC are represented in Table 1.

3.3. Disk diffusion antifungal test

Among 12 compounds tested, **1d** had a punctuate effect on *C. glabrata*, presenting an inhibition halo on the petri dish surface of approximately 10.6 mm, as suggested in Fig. 1A. Notably, **1j** exhibited a significantly mild inhibitory effect only for *C. glabrata* and *C. krusei*. The rest of the pyrazoles showed no zones of inhibition. However, the zones of inhibition for ketoconazole were more significant than all pyrazoles.

Table 1
Values of minimum inhibitory concentration (MIC) in μg/mL of novel pyrazoles compare with ketoconazole by CLSI reference methodology.

COMPOUNDS	*Candida parapsilosis ATCC 22019*	*Candida krusei ATCC 6258*	*Candida albicans ATCC 24433*	*Candida albicans ATCC 14053*	*Candida glabrata ATCC MYA 2950*
1a	>500	>500	>500	>500	500
1b	>500	>500	>500	>500	500
1c	500	500	>500	>500	500
1d	**>500**	**500**	**500**	**>500**	**500**
1e	>500	>500	>500	>500	500
1f	>500	>500	>500	>500	500
1g	>500	>500	>500	>500	500
1h	>500	>500	>500	>500	>500
1i	>500	>500	>500	>500	500
1j	**500**	**500**	>500	>500	**250**
1k	>500	>500	>500	>500	500
1l	>500	>500	>500	>500	250
KETOCONAZOLE	**3,1**	**15,65**	**62,5**	**62,5**	**125**

The detailed results of this test are exhibited in Fig. 1B and C.

3.4. Cytotoxicity activity and CC_{50} in vitro

To determine the CC_{50} of pyrazoles, we performed cytotoxicity tests on bone marrow macrophages using the resazurin assay. The CC_{50} values of the pyrazolic compounds and ketoconazole were determined by non-linear regression. The results confirm that most compounds showed lower cytotoxicity than ketoconazole (CC_{50} = 30.25 μg/mL), except **1c** (28 μg/mL), which resulted more toxic as presented in Table 2. **1d** had a cytotoxic effect lower since we got higher value of 57 μg/mL, as demonstrated in Fig. 2. These results were expected since ketoconazole and other first-generation azoles have been widely reported for hepatotoxicity and numerous side effects [34]. However, **1d** showed a promising effect with lower toxicity in primary cells.

To acquire further information about the cytotoxic activity, we employed the compound **1d** in the L929 fibroblast culture. We performed a cytotoxicity assay by resazurin to estimate cell viability based on mitochondrial metabolic activity [29]. The CC_{50} values were analyzed by non-linear regression. The results confirm that compound **1d** inhibited 50% of the population at 26 μg/mL. At the same time, ketoconazole showed a CC_{50} at 7.3 μg/mL, suggesting a lower toxic effect than the reference drug, as presented in Fig. 3.

3.5. Determination of the effect of respiratory inhibitors on susceptibility

It has been reported when one of the mitochondrial respiratory complexes is inhibited, and *Candida* spp can induce the oxidase alternative pathway that confers high tolerance to antifungals [10]. On the other hand, it has also been described that species with respiratory deficiency become more susceptible [11]. Six inhibitors of mitochondrial

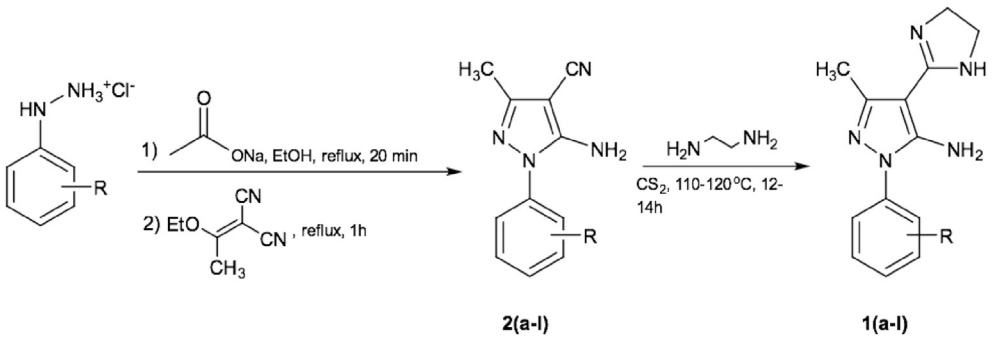

Scheme 1. Synthetic route to obtain **1(a–l)**.

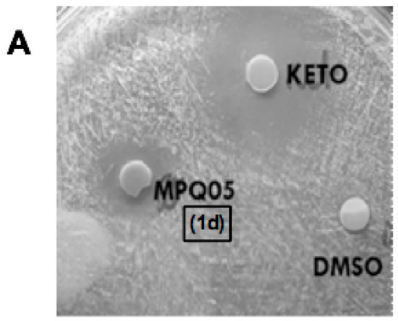

B

Table 2. Inhibition halos for pyrazoles in the disk diffusion antifungal test against *Candida* spp.

DERIVATIVES	*C. albicans* ATCC 24433	*C. albicans* ATCC 14053	*C. krusei* ATCC 6258	*C. glabrata* ATCC MYA 2950	*C. parapsilosis* ATCC 22019
1a	-	-	-	-	-
1b	-	-	-	-	-
1c	-	-	-	-	-
1d	-	-	-	10,6 mm	-
1e	-	-	-	-	-
1f	-	-	-	-	-
1g	-	-	-	-	-
1h	-	-	-	-	-
1i	-	-	8,5 mm	7 mm	-
1j	-	-	-	-	-
1k	-	-	-	-	-
Ketoconazole	33 mm	14,3 mm	25 mm	18,3 mm	26 mm

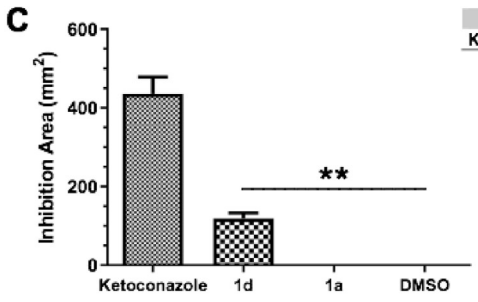

Fig. 1. Antifungal susceptibility tests by disk diffusion method. (A) Zone of inhibition on plate agar dish, (B) Diameters of inhibition halos for pyrazoles against *Candida* spp. (C) represents the mean of the inhibition area obtained with the compound **1d** in *C. glabrata* MYA 2950. The data indicate these two compounds as statistically superior to the DMSO control ($p < 0.05$); there is no statistical significance between them, and both were inferior to ketoconazole.

Table 2
Determination of CC_{50} on marrow bone macrophages. The values presented correspond to the concentration capable of inhibiting 50% of the population ±SD.

Compounds	CC_{50}/24 h
1b	39,24 ± 1,40
1c	27,29 ± 3,28
1d	56,84 ± 2,27
1e	48,28 ± 1,43
Ketoconazole	30,25 ± 2,27

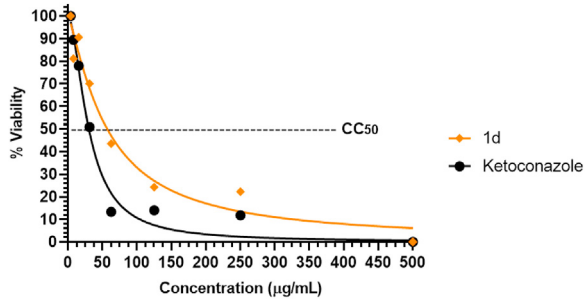

Fig. 2. Determination of CC_{50} of **1d** and ketoconazole on bone marrow cells. The values were normalized based on untreated control. A control with DMSO was tested (data not shown). This result reflects two experiments on two different days, performed in triplicates.

respiratory complexes were evaluated to validate these hypotheses. Sodium Azide was excluded from the study due to interference with the fluorescence indicator. As shown in Fig. 4, the fluorescence values of untreated control were normalized as 100% viability. Approximately 80% of viability was obtained in cells treated with Rotenone, Antimycin A(AA), Oligomycin A (OA), Potassium cyanide (CNK). However, the malonate had the lowest percentage of viability (in turn of 70%). After incubation, wells treated with inhibitors changed the color of the indicator as well as the untreated. Despite this, the values can be attributed to inhibitor action affecting the mitochondria and resazurin metabolization in this organelle. Although rotenone had a poor effect on yeast viability (80%) compared to the untreated control, we selected this complex I inhibitor because complex I inhibition may be less aggressive than the inhibition of complexes III and IV. Some authors suggested that inhibition of complex I did not participate in programmed cell death induced by rotenone [35,36]. Thus, rotenone has been used previously in combination with antifungals and studied in several studies about pathology on humans such as Parkinson disease [15].

The determination was performed according to the MIC protocol previously described with the addition of 0.05 mM rotenone. MIC value of <3.1 µg/ml was obtained for **1d** derivatives, which is much lower than the value obtained without inhibitor. A control with ketoconazole + rotenone was performed. It was also obtained a MIC of <3.1 µg/mL, as reported in Table 3. The same result was obtained with compound **1k** (data not shown). We demonstrate that pyrazole derivatives have a much stronger antifungal effect against *Candida* spp. when the complex I inhibitor rotenone is added to the culture.

Additionally, crescent rotenone concentrations continually exposed for 24 h on mice peritoneal macrophages did not cause toxicity in the range from 0.1 ng/mL to 1 µg/mL. The CC_{50} value calculated for rotenone was of 19.5 µg/mL (Fig. 5).

3.6. Measurement of intracellular ROS

Azoles have been reported to stimulate the production of peroxide, superoxide, and hydroxyl ions that damage membrane lipids [9,34]. In order to explain the possible mechanism of **1d** in *C. glabrata* observed in the disk diffusion test, we employed DHE, a fluorescence indicator, to quantify the production of intracellular ROS. **1d** and ketoconazole in sub-inhibitory concentrations (65 µg/mL) stimulated total intracellular ROS production. Both compounds exhibited a significantly higher ROS concentration than the untreated control after 2 h of incubation (Fig. 6). However, we observed lower ROS levels when tested with the highest ketoconazole and **1d** (500 µg/mL) concentrations. Interestingly, the treatment with **1d** + ketoconazole (65 µg/mL) showed a higher production of superoxide and ROS than untreated cells ketoconazole alone, suggesting a possible synergistic or additive effect. Rotenone 40 µg/mL

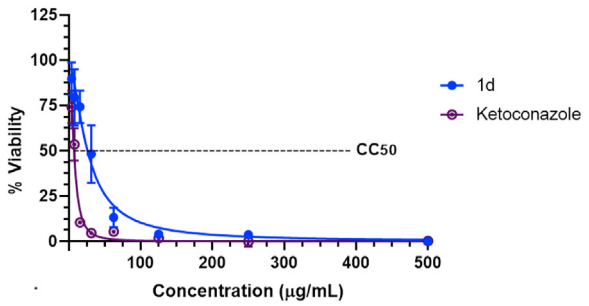

Fig. 3. Determination of CC_{50} of **1d** and ketoconazole on L929 fibroblasts. The values were normalized based on untreated control. In addition, a control with DMSO was tested (data not shown). Thus, this result reflects two experiments on two different days, performed in triplicates.

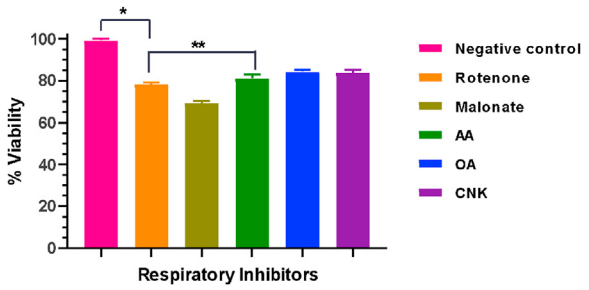

Fig. 4. Effect of respiratory inhibitors on a *C. albicans* culture. The percentage of viability was obtained from fluorescence units in every treatment. The data from untreated control was considered as 100% viability. We used 0.05 mM Rotenone; the significance levels between the groups are represented as: (*) $p <$ 0.0001 compared with the untreated control. However, there is no difference between Rotenone and Antimycin A (**) $p < 0.0776$.

Table 3
Values of minimum inhibitory concentration (MIC) in µg/mL of novel pyrazoles with rotenone 0.05 mM added to compare with MICs without rotenone. This result reflects two experiments on two different days, performed in triplicates.

COMPOUNDS	*C. albicans ATCC 14053* (µg/mL)	*C. glabrata*
1d	>500	500
1d + ROTENONE	<3.1	<3.1
KETOCONAZOLE	62.5	ND
KETOCONAZOLE + ROTENONE	<3.1	ND
ROTENONE 0.05 mM	+++	+++

ND: Not determined; +++: Growth; —: No Growth.

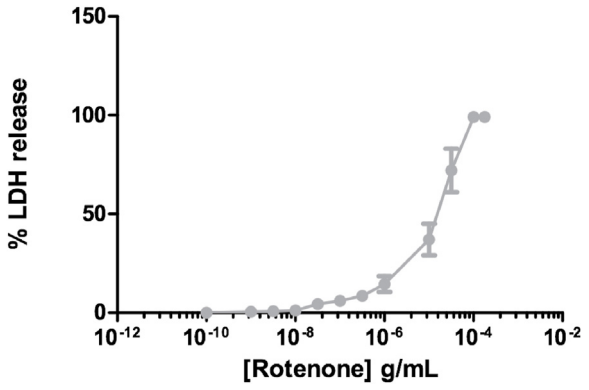

Fig. 5. Determination of CC_{50} of **rotenone** on mice peritoneal macrophages. The values were normalized based on Triton-X 100 detergent (0.1%) control. A control with DMSO was tested (data not shown). This result reflects three experiments on three different days, performed in triplicates.

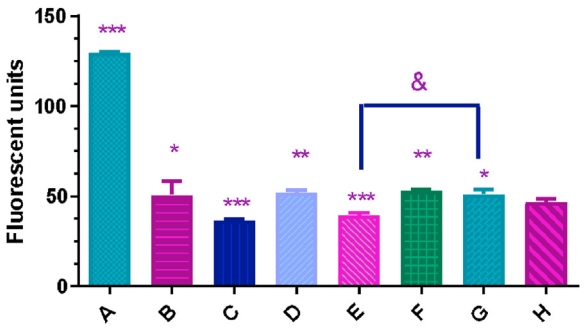

Fig. 6. Effect of pyrazoles on the production of **ROS** in *Candida glabrata*. (A) Rotenone 40 µg/mL, (B) AmB 65 µg/mL, (C) **1d** 500 µg/mL, (D) **1d** 65 µg/mL, (E) Ketoconazole 500 µg/mL, (F) Ketoconazole 65 µg/mL, (G) Ketoconazole + **1d** 65 µg/mL, (H) Untreated Cells. All data are represented with the mean ± Deviation. Fluorescence was detected with a DHE indicator. Rotenone was used as a positive control. The figure was made with information from two 2-h experiments done on different days under the same protocol. Statistical analysis is done through ANOVA. The levels of significance between the groups are represented as: (*) $p<0.05$, (**) $p<0.01$, (***) $p<0.001$ comparing with the untreated group, and *&* $p<0.05$ with the group treated with ketoconazole.

used as a positive control worked efficiently, reached the highest value with 40 fluorescent units; meanwhile, treatment with Amphotericin B produced the same levels as ketoconazole (Fig. 6).

Rotenone dramatically decreases the viability in plates with **1d** even when rotenone alone did not inhibit fungal growth. In order to investigate a possible synergistic action, we measured the total intracellular ROS. Paradoxically, **1d** + rotenone did not stimulate the formation of ROS. This treatment showed a significantly lower fluorescence production than **1d** alone ($p < 0.0008$), as shown in Fig. 7. Rotenone 0.05 mM alone (suggested concentration) decreased the total ROS compared to untreated cells. An element is probably related to complex I inhibition because this protein is the leading producer of ROS in mammalian cells [10,37,38]. Rotenone 0.05 mM stopped this complex partially, preventing the cell from accumulating ROS, opposite was treated with 40 µg/mL rotenone.

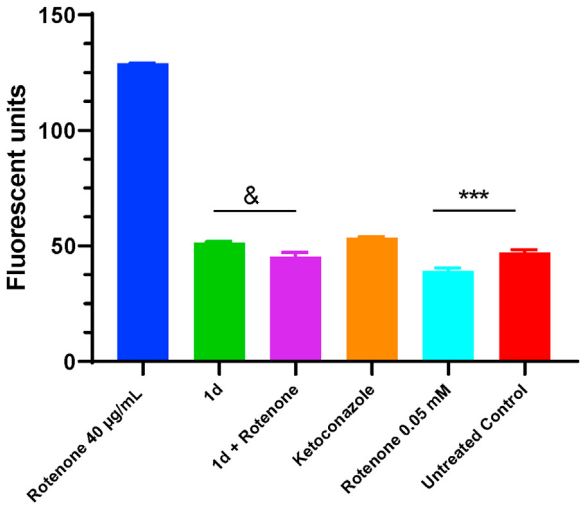

Fig. 7. Effect of **1d** with rotenone on the production of **ROS** in *Candida glabrata*. We used a 62.5 µg/mL concentration for **1d** and Ketoconazole; Rotenone 0.05 mM was added. Rotenone 40 µg/mL was used as a positive control. All data are represented with the mean ± SD. Fluorescence was detected with a DHE indicator. The figure was made with information from two 2-h experiments performed on different days under the same protocol. Statistical analysis is done through ANOVA. (&)**1d** produced more ROS than **1d** + Rotenone $p < 0.0008$. (***) Rotenone 0.05 µg/mL generated lower ROS than the untreated control $p < 0.0002$.

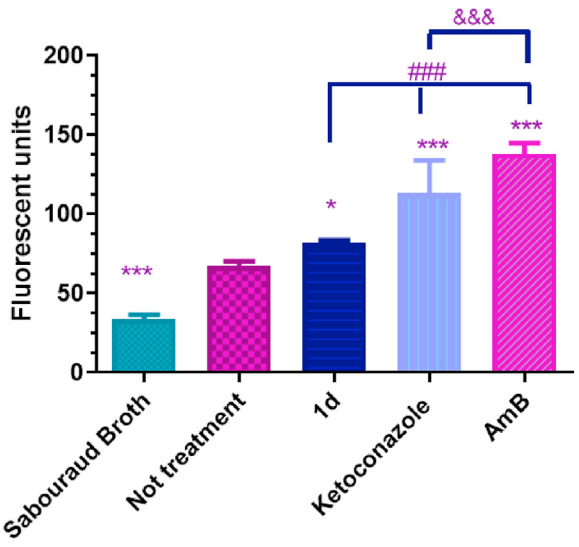

Fig. 8. Determination of the type of antifungal action of **1d** Ketoconazole was used as a fungistatic control and Amphotericin B as a fungicidal control. All data are represented with the mean ± s.d. Fluorescence was detected with an ethidium bromide indicator. The figure was made with information from two 24-h incubation experiments realized on different days under the same protocol. Statistical analysis is done through ANOVA. The levels of significance between the groups are represented as: (*) $p < 0.05$, $p < 0.001$ (***) comparing with the untreated group and ###$p < 0.001$ with the group treated with **1d** and &&&$p < 0.001$ compared to ketoconazole.

3.7. Determination of fungistatic or fungicidal activity

In general, the azole family, including those triazoles, has been described as fungistatic by targeting the enzyme lanosterol 14α demethylase (Erg11p or Cytochrome P450) responsible for the synthesis of ergosterol [1,4]. To understand the possible fungistatic or fungicidal effect of pyrazoles, we treated the fluorescence of non-viable cells with 50 nM ethidium bromide. This indicator has a molecular weight of 329 Da and a positive charge. Thus, ethidium is impermeable to the fungal membrane, and consequently, there is low fluorescence levels emission. However, events causing a rupture in the fungal membrane increase the dye entry and binding to DNA.

In consequence, there is an increase in the emission of its fluorescence [39]. In Fig. 8, Amphotericin B reached approximately 150 Fluorescent units, a value higher than Ketoconazole and **1d** with 120 and 80 Fluorescent units. The Amphotericin B result was expected because of its mechanism of action, in fact amphotericin B pore or ionic channels formation in the plasma membrane [40]. So derivative **1d** produced an increase in ethidium bromide uptake, indicating antifungal activity. However, when compared to the positive control, Amphotericin B, this effect was modest. **1d** acts in a mostly fungistatic manner.

It was also evaluated the fluorescence due to the combination of **1d** + rotenone which resulted higher than that **1d** alone ($p < 0.0281$) as shown in Fig. 9A and B suggesting that the possible synergistic effect among them potentiates the fungicidal action against *C. glabrata*. However, treatment with ketoconazole maintains the highest fluorescent units from non-viable cells in this experiment (Fig. 9B).

We expected that the increase in fluorescence due to cell death resulted from the ROS accumulation by dysfunction of Mitochondrial Complex I as widely reported. However, although the fungicidal effect increased, ROS level decreased with rotenone 0.05 mM treatment, paradoxically (Fig. 7).

Complex I is an NADH: Ubiquinone oxidoreductase is a protein responsible for pumping protons from the mitochondrial matrix for NADH oxidation and is essential for the mitochondrial respiratory chain and ATP synthesis. This complex is sensitive to rotenone [37]. Meanwhile, fungi have alternative NADH Oxidoreductases that are not inhibited by the presence of rotenone and do not contribute to increased ROS [10]. Therefore, rotenone 0.05 mM partially inhibits complex I, limiting ATP production to induce pro-survival cellular processes in the presence of pyrazole and leading to cell death. However, a possible mechanism needs to be elucidated since this data cannot be attributed to high ROS accumulation.

4. Conclusion

Among the 12 pyrazole derivatives synthetized and tested, only two presented low-mild antifungal effects, **1d** and **1k**. For that reason, we decided to treat yeast with an adjuvant to enhanced inhibitory activity. In this study, we used rotenone as an adjuvant in the action of pyrazoles. Rotenone was chosen to determine the effect of respiration inhibitors since there are reliable studies in the pharmaceutical industry for the treatment of patients. No toxic effect was observed after the treatment for 24 h in tested concentrations. The results indicate that this inhibitor helps to potentiate the effect of the novel tested pyrazole derivatives as MIC values abruptly decreased to <3.1 μg/mL. Many studies attribute the synergistic effect of rotenone with other compounds to high concentrations of ROS. We corroborate this phenomenon by treating the cells with a high dose used as a control (40 μg/mL). However, the concentration suggested for the combined treatment with **1d** reduced the ROS production compared to untreated cells control. ATP levels and oxygen consumption may help to elucidate this synergistic action.

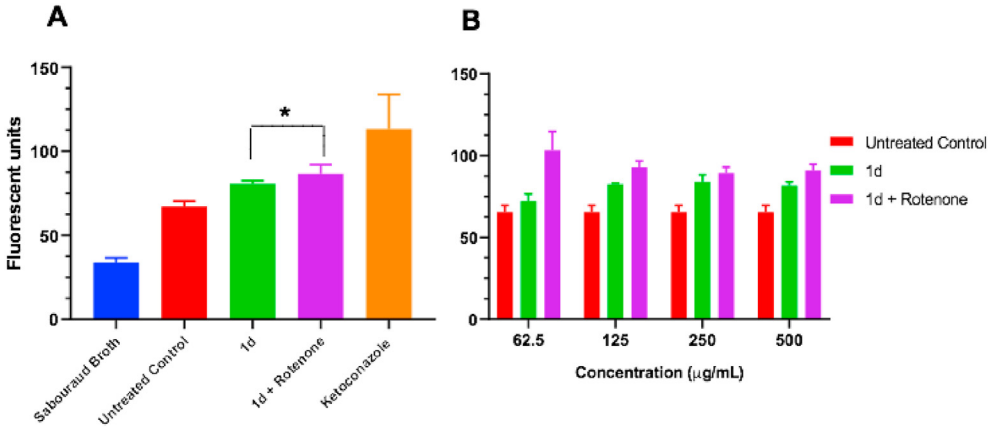

Fig. 9. Determination of the effect of **1d** with rotenone on the viability of *Candida glabrata*. (A) We used in a concentration of 500 μg/mL **1d** for every treatment; Rotenone 0.05 mM was added. Ketoconazole 500 μg/mL was used as a positive control and a drug-free treatment as a negative control. All data are represented with the mean ± SD. Fluorescence was detected with an ethidium bromide indicator. **1d** + Rotenone showed better antifungal action on yeast viability than **1d** alone (*) $p < 0.0281$; Ketoconazole had the higher fluorescent units than **1d** + Rotenone (**) $p < 0{,}0120$. (B) Fluorescent units from an experiment with 62.5–500 μg/mL concentrations of **1d** with or without rotenone. The figure was made with information from two 2-h incubation experiments carried out on different days under the same protocol. Statistical analysis is done through ANOVA.

This study provides a complete overview of the functionality of pyrazole derivatives, presenting them as an alternative for antifungal treatment with certain concentration limits, considering the parameters necessary to assess toxicity and safety issues.

Declaration of interests

The authors declare that they have no known competing financial interests or personal relationships that could have appeared to influence the work reported in this paper.

Acknowledgment

The authors want to thanks to the Program for Technological Development in Tools for Health-RPT of Instituto Oswaldo Cruz, Fiocruz, Rio de Janeiro and source of financing provided by CAPES and CNPq.

Appendix A. Supplementary data

Supplementary data to this article can be found online at https://doi.org/10.1016/j.ejmcr.2022.100045.

References

[1] M. Sanguinetti, B. Posteraro, C. Lass-Flörl, Antifungal drug resistance among *Candida* species: mechanisms and clinical impact, Mycoses 58 (2015) 2–13, https://doi.org/10.1111/myc.12330.

[2] J.P. Richardson, D.L. Moyes, J. Ho, J.R. Naglik, Candida innate immunity at the mucosa, Semin. Cell Dev. Biol. 89 (2019) 58–70, https://doi.org/10.1016/j.semcdb.2018.02.026.

[3] M.C. Arendrup, Candida and Candidaemia. Susceptibility and Epidemiology, Dan Med J 1–32 (2013). PMID: 24192246.

[4] A. Mane, P. Vidhate, C. Kusro, V. Waman, V. Saxena, U. Kulkarni-Kale, A. Risbud, Molecular mechanisms associated with Fluconazole resistance in clinical *Candida albicans* isolates from India, Mycoses 59 (2016) 93–100, https://doi.org/10.1111/myc.12439.

[5] M. Nucci, F. Queiroz-Telles, T. Alvarado-Matute, I.N. Tiraboschi, J. Cortes, J. Zurita, M. Guzman-Blanco, M.E. Santolaya, L. Thompson, J. Sifuentes-Osornio, J.I. Echevarria, A.L. Colombo, Epidemiology of candidemia in Latin America: a laboratory-based survey, PLoS One 8 (2013). https://doi.org/10.1371/journal.pone.0059373.

[6] S. Silva, M. Negri, M. Henriques, R. Oliveira, D.W. Williams, J. Azeredo, *Candida glabrata, Candida parapsilosis* and *Candida tropicalis*: biology, epidemiology, pathogenicity, and antifungal resistance, FEMS Microbiol. Rev. 36 (2012) 288–305. https://doi.org/10.1111/j.1574-6976.2011.00278.x.

[7] D.S. Perlin, R. Rautemaa-Richardson, A. Alastruey-Izquierdo, The global problem of antifungal resistance: prevalence, mechanisms, and management, Lancet Infect. Dis. 17 (2017) 383–392, https://doi.org/10.1016/S1473-3099(17)30316-X.

[8] A.C. Mesa-Arango, N. Trevijano-Contador, E. Román, R. Sánchez-Fresneda, C. Casas, E. Herrero, J.C. Argüelles, J. Pla, M. Cuenca-Estrella, O. Zaragoza, The production of reactive oxygen species is a universal action mechanism of Amphotericin B against pathogenic yeasts and contributes to the fungicidal effect of this drug, Antimicrob. Agents Chemother. 58 (2014) 6627–6638, https://doi.org/10.1128/AAC.03570-14, 2014.

[9] G.F. Ferreira, L. Baltazar, J.R. Santos, A.S. Monteiro, L.A. Fraga, M.A. Resende-Stoianoff, D.A. Santos, The role of oxidative and nitrosative bursts caused by azoles and amphotericin B against the fungal pathogen *Cryptococcus gattii*, J. Antimicrob. Chemother. 68 (2013) 1801–1811, https://doi.org/10.1093/jac/dkt114.

[10] E.J. Helmerhorst, M.P. Murphy, R.F. Troxler, F.G. Oppenheim, Characterization of the mitochondrial respiratory pathways in *Candida albicans*, Biochim. Biophys. Acta 1556 (2002) 73–80, https://doi.org/10.1016/S0005-2728(02)00308-0.

[11] Y. Peng, D. Dong, C. Jiang, B. Yu, X. Wang, Y. Ji, Relationship between respiration deficiency and azole resistance in clinical *Candida glabrata*, FEMS Yeast Res. 1 (2012) 719–727, https://doi.org/10.1111/j.1567-1364.2012.00821.x.

[12] C. Wirth, U. Brandt, C. Hunte, V. Zickermann, Structure and function of mitochondrial complex I, Biochim. Biophys. Acta 1857 (2016) 902–914, https://doi.org/10.1016/j.bbabio.2016.02.013.

[13] A. Castro, C. Lemos, A. Falca, A.S. Fernandes, N.L. Glass, A. Videira, Rotenone enhances the antifungal properties of staurosporine, Eukaryot. Cell 9 (6) (2010) 906–914, https://doi.org/10.1128/EC.00003-10, 2010.

[14] Q. Ai, Y. Jing, R. Jiang, L. Lin, J. Dai, Q. Che, D. Zhou, M. Jia, J. Wan, L. Zhang, Rotenone, a mitochondrial respiratory complex I inhibitor, ameliorates lipopolysaccharide/D-galactosamine-induced fulminant hepatitis in mice, Int. Immunopharm. 21 (2014) 200–207, https://doi.org/10.1016/j.intimp.2014.04.028.

[15] L.V. Darbinyan, L.E. Hambardzumyan, K.V. Simonyan, V.A. Chavushyan, L.P. Manukyan, V.H. Sarkisian, Rotenone impairs hippocampal neuronal activity in a rat model of Parkinson's disease, Pathophysiology 24 (2017) 23–30, https://doi.org/10.1016/j.pathophys.2017.01.001, 2017.

[16] M. Shamoto-Nagai, W. Maruyama, Y. Kato, K. Isobe, M. Tanaka, M. Naoi, T. Osawa, An inhibitor of mitochondrial complex I, Rotenone, inactivates proteasome by oxidative modification and induces aggregation of oxidized proteins in SH-SY5Y cells, J. Neurosci. Res. 74 (2003) 589–597, https://doi.org/10.1002/jnr.10777.

[17] J.V. Faria, P.F. Vegi, A. Miguita, M.S. Dos Santos, N. Boechat, A. Bernardino, Recently reported biological activities of pyrazole compounds, Bioorg. Med. Chem. 25 (2017) 5891–5903, https://doi.org/10.1016/j.bmc.2017.09.035.

[18] A.M. Vijesh, A.M. Isloor, S. Telkar, S.K. Peethambar, S. Rai, Synthesis, characterization, and antimicrobial studies of some new pyrazole incorporated imidazole derivatives, Eur. J. Med. Chem. 46 (2011) 3531–3536, https://doi.org/10.1016/j.ejmech.2011.05.005.

[19] S. Oliveira, L. Pizzuti, F. Quina, A. Flores, R. Lund, C. Lencina, B.S. Pacheco, C.M. De Pereira, E. Piva, Anti-Candida, anti-enzyme activity and cytotoxicity of 3,5-Diaryl-4,5-dihydro-1H-pyrazole-1-carboximidamides, Molecules 19 (2014) 5806–5820, https://doi.org/10.3390/molecules19055806.

[20] H. B'Bhatt, S. Sharma, Synthesis and antimicrobial activity of pyrazole nucleus containing 2-thioxothiazolidin-4-one derivatives, Arab. J. Chem. 10 (2017) 1590–1596, https://doi.org/10.1016/j.arabjc.2013.05.029.

[21] M. Abdel-Aziz, G. el-D.A. Abuo-Rahma, A.A. Hassan, Synthesis of novel pyrazole derivatives and evaluation of their antidepressant and anticonvulsant activities, Eur. J. Med. Chem. 44 (2009) 3480–3487, https://doi.org/10.1016/j.ejmech.2009.01.032.

[22] İ. Koca, A. Özgür, K.A. Coşkun, Y. Tutar, Synthesis and anticancer activity of acyl thioureas bearing pyrazole moiety, Bioorg. Med. Chem. 21 (2013) 3859–3865, https://doi.org/10.1016/j.bmc.2013.04.021.

[23] K.M. Dawood, T.M.A. Eldebss, H.S.A. El-Zahabi, M.H. Yousef, P. Metz, Synthesis of some new pyrazole-based 1,3-thiazoles and 1,3,4-thiadiazoles as anticancer agents, Eur. J. Med. Chem. 70 (2013) 740–749, https://doi.org/10.1016/j.ejmech.2013.10.042.

[24] K. Karrouchi, S. Radi, Y.R. Id, J. Taoufik, Synthesis and pharmacological activities of pyrazole derivatives: a review, Molecules 23 (2018) 134, https://doi.org/10.3390/molecules23010134.

[25] S. Mert, R. Kasımoğulları, T. İça, F. Çolak, A. Altun, S. Ok, Synthesis, structure-activity relationships, and in vitro antibacterial and antifungal activity evaluations of novel pyrazole carboxylic and dicarboxylic acid derivatives, Eur. J. Med. Chem. 78 (2014) 86–96, https://doi.org/10.1016/j.ejmech.2014.03.033.

[26] A.M. Vijesh, A.M. Isloor, P. Shetty, S. Sundershan, H. Kun, New pyrazole derivatives containing 1,2,4-triazoles and benzoxazoles as potent antimicrobial and analgesic agents, Eur. J. Med. Chem. actions. 62 (2013) 410–415, https://doi.org/10.1016/j.ejmech.2012.12.057.

[27] V.J. Boyle, M.E. Fancher, R.W.J. Ross, Rapid, modified Kirby-Bauer susceptibility test with single, high-concentration antimicrobial disks, Antimicrob. Agents Chemother. 3 (1973) 418–424, https://doi.org/10.1128/aac.3.3.418.

[28] Clinical and Laboratory Standards Institute/NCCLS, Performance Standards for Antimicrobial Susceptibility Testing, Clinical and Laboratory Standards Institute, 940 West Valley Road, Suite 1400, Fifteenth Informational Supplement. CLSI/NCCLS document M100-S15, Wayne, Pennsylvania 19087-1898 USA, 2005, ISBN 1-56238-556-9.

[29] S.N. Rampersad, Multiple applications of alamar blue as an indicator of metabolic function and cellular health in cell viability bioassays, Sensors 12 (2012) 12347–12360, https://doi.org/10.3390/s120912347.

[30] J. O'Brien, I. Wilson, T. Orton, F. Pognan, Investigation of the Alamar Blue (resazurin) fluorescent dye for the assessment of mammalian cell cytotoxicity, Eur. J. Biochem. 267 (2000) 5421–5426, https://doi.org/10.1046/j.1432-1327.2000.01606.x.

[31] R.X. Faria, D.T.G. Gonzaga, P.A.F. Pacheco, A.L.A. Souza, V.F. Ferreira, F.de C. da Silva, Searching for new drugs for Chagas diseases: triazole analogs display high in vitro activity against *Trypanosoma cruzi* and low toxicity toward mammalian cells, J. Bioenerg. Biomembr. 50 (2018) 81–91, https://doi.org/10.1007/s10863-018-9746-z.

[32] J.V. Faria, M.S. Dos Santos, A.M.R. Bernardino, K.M. Becker, G.M.C. Machado, R.F. Rodrigues, M.M. Canto-Cavalheiro, L.L. Leon, Synthesis and activity of novel tetrazole compounds and their pyrazole-4-carbonitrile precursors against Leishmania spp, Bioorg. Med. Chem. Lett 23 (2013) 6310–6312, https://doi.org/10.1016/j.bmcl.2013.09.062.

[33] M.S. dos Santos, M.L. Oliveira, A.M. Bernardino, R.M. de Léo, V.F. Amaral, F, F.T. de Carvalho, L.L. Leon, M.M. Canto-Cavalheiro, Synthesis and antileishmanial evaluation of 1-aryl-4-(4,5-dihydro-1H-imidazole-2-yl)-1H-pyrazole derivatives, Bioorg. Med. Chem. Lett 21 (2011) 7451–7454. https://doi.org/10.1016/j.bmcl.2011.09.134.

[34] J. Houšť, J. Spížek, V. Havlíček, Antifungal Drugs, *Metabolites* 10 (2020) 106, https://doi.org/10.3390/metabo10030106.

[35] W.S. Choi, S.E. Kruse, R.D. Palmiter, Z. Xia, Mitochondrial complex I inhibition is not required for dopaminergic neuron death induced by rotenone, MPP+, or paraquat, Proc. Natl. Acad. Sci. U. S. A 105 (2008) 15136–15141, https://doi.org/10.1073/pnas.0807581105.

[36] D. Li, H. Chen, A. Florentino, D. Alex, P. Sikorski, W.A. Fonzi, R. Calderone, Enzymatic dysfunction of mitochondrial complex I of the *Candida albicans* Goa1 mutant is associated with increased reactive oxidants and cell death, Eukaryot. Cell 10 (2011) 672–682, https://doi.org/10.1128/EC.00303-10.

[37] T. Joseph-horne, D.W. Hollomon, P.M. Wood, Fungal respiration: a fusion of standard and alternative components, Biochim. Biophys. Acta 1504 (2001) 179–195, https://doi.org/10.1016/s0005-2728(00)00251-6.

[38] M. Forkink, F. Basit, J. Teixeira, H.G. Swarts, W.J.H. Koopman, P.H.G.M. Willems, Redox Biology Complex I and complex III inhibition speci fi cally increase cytosolic

hydrogen peroxide levels without inducing oxidative stress in HEK293 cells, Redox Biol. 6 (2015) 607–616, https://doi.org/10.1016/j.redox.2015.09.003.
[39] D.W. Gray, P.J. Morris, The use of fluorescein diacetate and ethidium bromide as a viability stain for isolated islets of Langerhans, Stain Technol. 62 (1987) 373–381, https://doi.org/10.3109/10520298709108028.
[40] Y.J. Rodriguez, L.F. Quejada, J.C. Villamil, Y. Baena, C.M. Parra-Giraldo, L.D. Perez, Development of amphotericin B micellar formulations based on copolymers of poly(ethylene glycol) and poly(ε-caprolactone) conjugated with retinol, Pharmaceutics 12 (2020) 196, https://doi.org/10.3390/pharmaceutics12030196.